GHGT-11

Monitoring of CCS Areas using Micro Unmanned Aerial Vehicles (MUAVs)

P. P. Neumann[a],*, S. Asadi[b], V. Hernandez Bennetts[b], A. J. Lilienthal[b], and

M. Bartholmai[a]

[a]BAM Federal Institute for Materials Research and Testing, Unter den Eichen 87, 12205 Berlin, Germany
[b]Center for Applied Autonomous Sensor Systems, Örebro University, 70182 Örebro, Sweden

Abstract

Carbon capture & storage (CCS) is one of the most promising technologies for greenhouse gas (GHG) management. However, an unsolved issue of CCS is the development of appropriate long-term monitoring systems for leak detection of the stored CO_2. To complement already existing monitoring infrastructure for CO_2 storage areas, and to increase the granularity of gas concentration measurements, a quickly deployable, mobile measurement device is needed. In this paper, we present an autonomous gas-sensitive micro-drone, which can be used to monitor GHG emissions, more specifically, CO_2. Two different measurement strategies are proposed to address this task. First, the use of predefined sensing trajectories is evaluated for the task of gas distribution mapping using the micro-drone. Alternatively, we present an adaptive strategy, which suggests sampling points based on an artificial potential field (APF). The results of real-world experiments demonstrate the feasibility of using gas-sensitive micro-drones for GHG monitoring missions. Thus, we suggest a multi-layered surveillance system for CO_2 storage areas.

Keywords: gas-sensitive micro-drone; gas distribution mapping; sensor planning; artificial potential field; CCS;

1. Introduction

The release of GHG is an acute threat mainly responsible for extensive ecological damages such as ozone layer depletion and global warming. The main source of CO_2 emissions is the fossil fuel consumption in industry and transportation [1]. Thus, new technologies have to be developed to mitigate the CO_2 emissions into the atmosphere. CCS is one of the most promising technologies for GHG control and reduction. However, one of the main unsolved issues of CCS is the development of appropriate long-

---

* Corresponding author. Tel.: +49-30-8104-3629; fax: +49-30-8104-1917.
E-mail address: patrick.neumann@bam.de.

Fig. 1. Micro-drone equipped with gas-sensitive payload in flight.

term monitoring systems for the leakage detection of the stored CO_2 [1]. A fundamental requirement for leakage control is the availability of measurements of relevant gas concentrations in areas of interest with high spatial and temporal granularity. In order to obtain a truthful representation of the gas distribution, it is essential to collect a set of spatially distributed measurements of relevant variables such as gas concentration and wind information. For economical and logistic reasons, a dense stationary sensor network is in many cases not a viable solution. To complement state-of-the-art monitoring systems for CO_2 storage areas [2] and to enhance the spatial resolution of gas measurements, a quickly deployable, mobile measurement device is needed for leakage monitoring. Therefore, we suggest a multi-layered surveillance system for CO_2 storage areas.

In this work, we present a gas-sensitive micro-drone, which can be used to monitor GHG emissions, specifically CO_2. The structure of this paper is as follows: in Sec. 2, we present a gas-sensitive micro-drone, which is able to estimate the wind vector without a dedicated anemometer [3], [4]. In Sec. 3, we address the task of environmental monitoring with the micro-drone using predefined sensing trajectories or an adaptive sensor planning (SP) algorithm [3] where the next sampling location is selected based on the previously visited sampling locations and a continuously updated gas distribution model. Similar experiments with predefined sensing trajectories were presented in [3], [4]. In this paper, however, we present new experiments performed exclusively with CO_2. To model gas distribution, identify candidate locations at which a gas source may be present, and represent the degree of interest with which future measurements should be carried out at different locations, we use the Kernel DM+V/W algorithm [5]. Next, in Sec. 4, we present results of three sets of real-world experiments performed with the gas-sensitive micro-drone and demonstrate that the peak in the predictive variance in the created gas distribution model can provide a good estimate of the location of leakages. We then conclude in Sec. 5 with a discussion of the experimental results especially regarding use of the proposed system in CO_2 monitoring.

2. Gas-sensitive Micro-Drone

The Airrobot AR100-B micro-drone (Fig. 1) has a diameter of 1 *m* and is operated by four brushless electric motors. The maximum payload mass amounts to 200 *g* with a total flight mass of about 1.3 *kg*. The micro-drone was modified to incorporate gas-sensitive devices as payloads [3], [4]. An e-nose capable of accommodating four commercially available metal oxide (MOX) sensors and an electrochemical (EC) cell, as well as a commercially available gas detector (Dräger X-am 5600) can be used as gas-sensitive payloads. The latter device can be equipped with EC and IR gas sensors. The e-nose allows a sampling rate of 8 Hz for each sensor, whereas the Dräger gas detector allows a sampling rate of 1 Hz for each sensor. The maximum flight time is about 20 *min*. The micro-drone can withstand a maximum wind speed of 8 *m/s*. The flight control relies on an on-board inertial measurement unit (IMU) which consists of a three axis accelerometer and a three axis rotation rate sensor. Magnetic field sensor and GPS improve the accuracy of the IMU, and are used to compensate for the sensor drift. A barometric pressure sensor is used to control the altitude of the micro-drone. Communication with the ground station

is established by a wireless radio link. Data packets can include control instructions or data coming from the micro-drone's on-board sensing modalities. The operating distance of the remote control and communication link is 1 *km*. Due to the restrictions imposed by the platform; the micro-drone doesn't carry any wind sensing modalities. Instead, wind measurements are estimated by fusing different on-board sensing modalities to compute the parameters of the wind triangle [3]. The wind triangle is commonly used in aerial navigation and describes the relationships between the flight vector, the ground vector, and the wind vector. The micro-drone can be operated manually or in an autonomous GPS waypoint navigation.

3. Statistical Gas Distribution Modeling (GDM)

To build a predictive gas distribution model, we use the Kernel DM+V/W algorithm introduced by Reggente and Lilienthal [5]. The input to this algorithm is a set $D = \{(x_i, r_i, v_i)\}_{1 \leq i \leq n}$ of gas sensor measurements r_i and wind measurements v_i collected at locations x_i. The output is a grid model that computes a confidence estimate, as well as the distribution mean and variance for each cell k of the gridmap. The confidence estimate depends on the scaling parameter σ_Ω and indicates whether a large number of measurements are available in the close vicinity of the respective cell or not. We use the 2D version of the Kernel DM+V/W algorithm since the field of main application is surface monitoring, which demands 2D results. Thus, the micro-drone was kept in a single 2D plane during the experiments.

The Kernel DM+V/W algorithm models the information content of each measurement with a two-dimensional, bivariate Gaussian kernel N. The shape and orientation of this kernel depends on the local airflow vector v and on two meta-parameters σ and γ. If no wind is measured (or if no wind information is available), the Gaussian kernel has a circular shape that extends according to a spatial scale σ. In case of a non-zero wind measurement the kernel takes the shape of an elongated ellipse with the semi-major axis rotated in wind direction and stretched according to the strength of the wind and the wind scale γ. The elongated ellipse describes the additional information the system has about from which direction a sensed patch of gas came from and where it will move to in the immediate future.

3.1. GDM with Predefined Trajectories

Lilienthal and Duckett suggest in [6] (for a precursor of the Kernel DM+V/W algorithm) that, in order to build concentration gridmaps, it is required for the sensor's trajectory to roughly cover the search space and that measurements are taken from multiple directions. This can be achieved in a straightforward way by commanding a mobile robot to follow predefined trajectories that comply with the above mentioned requirements. In case of a micro-drone, which introduces sustainable disturbances to the environment that modifies the current gas distribution, it is not desirable to visit measurement positions more than once in a certain time period. Moving the micro-drone along a spiral is also problematic as the disturbance in the upwind part of the spiral could destroy the plume structure in its downwind part. In order to obtain more truthful gas distribution models, we decided to move the micro-drone in each experiment along a predefined sweeping trajectory preferably in upwind direction.

As a result, we expect to minimize the effect that the disturbances of the micro-drone has on the resulting gas distribution model. Furthermore, building detailed gas distribution maps over large areas is time consuming and the batteries of the micro-drone only provide power for approx. 20 *min*. Thus, performing just a single sweep is desirable for the above mentioned reasons.

3.2. GDM with Adaptive Sampling

To derive a truthful gas distribution model and to reduce the exploration time, we apply an adaptive sampling strategy based on the sensor planning (SP) approach presented in [3]. The basic SP algorithm uses information about the target area, previous sampling locations, and the current statistical gas distribution model and combines several objectives using a modified artificial potential field (APF) to plan where to collect the next samples. In particular, three objectives are used that direct the sensor towards areas of (1) high predictive mean and (2) high predictive variance, while (3) maximizing the coverage area. The first two objectives implement exploitation in areas with unusual gas concentration. The sensor is attracted by an APF, which is created by charges that are placed in each grid cell center. The strength of these charges is given by the corresponding predictive mean and variance of the gas distribution model. The third objective that corresponds to exploration is implemented by a repulsive potential generated by placing charges at all previous measurement locations, resulting in the third APF contribution. In the current implementation, we assign the same repulsive force to all previous measurements. Finally, the APF contributions are additively combined with importance factors β_M, β_V, and β_C for mean, variance, and coverage objectives, respectively. Next, in each sampling iteration, a total of n_{sp} suggested measurement points are identified by selecting the location at which the total APF takes its maximum and updating the APF by temporarily placing an additional measurement charge at the selected location. In this way the SP component distributes its suggestions over the target area without any spatial order. Moving the mobile gas sensor directly to these locations tends to create a seesaw movement, which empties the batteries sooner, resulting in fewer measurements. Therefore, we add a locality constraint by selecting the *most often suggested close-by* measurement location from the n_{sp} suggestions (rather than the first suggestion) [3]. A location far away from the current position will only be selected if it was suggested frequently.

4. Real-World Experiments

4.1. Experimental Environments and Setups

A total of three sets of experiments were performed. In the first two sets, the micro-drone was programmed to explore the experimental areas following a sweeping trajectory, whereas the adaptive SP algorithm with locality constraint was used in the last set of experiments.

The first set was performed in the botanic garden of Berlin over an area of 12 x 6 m^2. The step size of the micro-drone in x and y direction was set to 2.0 m. A CO_2 gas cylinder was used as the gas source and four fans were placed in the experimental area. The gas outlet was connected to the fan in order to spread the CO_2 away from the cylinder. Both, the e-nose and the gas-sensing payload were used successively, each equipped with CO_2 sensors. The CO_2 sensor of the e-nose is based on an EC cell (Figaro TGS4161; T_{90} = 1.5 min), whereas the Dräger X-am 5600 was equipped with an IR sensor ($T_{90} \leq 10$ s). The second set was performed in the geochemically active Tuscany Region (Italy) close to the village Bagni San Filippo. The trials were conducted over an area of 20 x 24 m^2. The step size in x and y direction was set to 4.0 m. Three visible, naturally bubbling CO_2 area sources were located within the experimental area as well as a zone of natural gas accumulation. The experiments were performed on two different days with different weather conditions (foggy vs. sunny). The third set was carried out in an 8 x 12 m^2 outdoor area at Örebro University and on the BAM Test Site 'Technical Safety' (BAM TTS) with the gas-sensing payload equipped with CO sensors (EC). A barbecue filled with burning coal and fresh, damp wood was used as a pollution source and was placed approx. in the middle of the experimental area.

Additionally, the following settings were made for each set of experiments: the flight speed of the micro-drone between the measurement positions was set to 1 m/s, the altitude was kept constant manually during the experiments, and at each measurement position, the micro-drone stopped to take gas

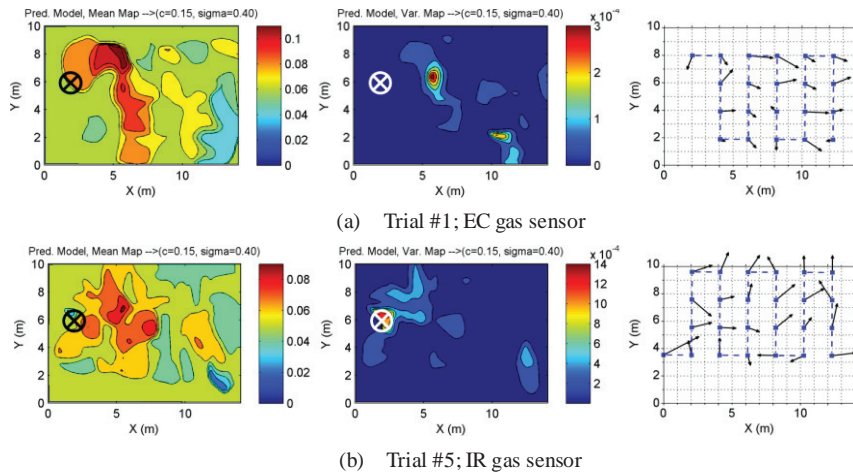(a)   Trial #1; EC gas sensor

(b)   Trial #5; IR gas sensor

Fig. 2. Botanic garden experiments: Predictive mean (left) and variance map (middle) of the gas distribution and the corresponding mean airflow map (right) and the path of the micro-drone of the (a) first and fifth trial created using Kernel DM+V/W. The gas source was located approx. at position (2, 6) *m* and is denoted by the cross. The starting position of the micro-drone is located approx. at position (a) (12, 2) *m* and (b) - (d) (12, 3.5) *m*. The concentration value of CO_2 is given in % by volume.

concentration and wind measurements for about 20 *s* with a sampling rate of 1 Hz. The micro-drone was set to autonomous waypoint mode directly after take-off.

4.2. Experimental Results

The sets of gas distribution maps presented in this section were created using the Kernel DM+V/W algorithm [5] with γ heuristically set to 0.2 *s* and a cell size of 0.15 *m*. The kernel width σ was also set heuristically and varied from 0.4 to 1.2 *m* depending on the experimental setup and the scaling parameter σ_Ω was set in a fixed relation to the kernel width σ. The smaller value of the kernel width was chosen when a dense set of measurements was available, whereas the larger value served to smooth the maps accordingly when only sparse measurements distributed over a large area were available. Generally, we wanted obtain high confidence over the whole experimental area and not only along the trajectory of the micro-drone due to an undersized chosen Gaussian kernel. Equal importance factors β_M, β_V, and β_C were chosen for the APF contributions.

Botanic garden experiments – Despite artificial ventilation, the wind conditions during all trials were very unstable. The average wind speed was between 1.0 and 1.4 *m/s* and the average wind direction changed between 91° and 172°. The circular variance lay around 0.55 and 0.78, which indicates that the wind vectors were highly spread. However, the produced gas distribution maps show that CO_2 could be dispersed in *x* direction using the four fans. Fig. 2 shows exemplary the results of trial #1, and #5 performed in the botanic garden of Berlin. Trial #1 was performed with the e-nose, whereas the gas-sensing payload was used in trial #5. The quantitative results remain more or less constant in the created maps, while the qualitative results differ more strongly. For instance, the produced predictive mean map of trial #1 does not allow to identify a plume structure. Instead, it seems that the sensor of the e-nose retains high measured concentrations for quite a long time due to the slow sensor recovery expanding most likely the local measurement to a much larger area with slowly decreasing concentration values following the sweeping movement of the micro-drone. This memory effect in the sensor response is not visible in trial #5 using the Dräger X-am 5600 as gas-sensing payload. In contrast to that, an intermittent

(a)   Trial #1; day 1
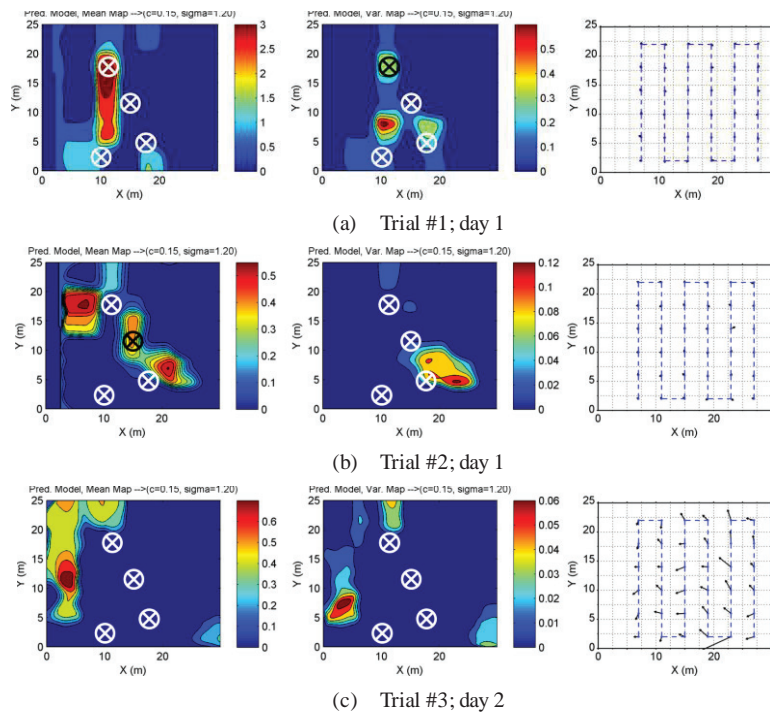

(b)   Trial #2; day 1

(c)   Trial #3; day 2

Fig. 3. Inferno experiments: Predictive mean (left) and variance map (middle) of the gas distribution of the (a) first, (b) second, and (c) third trial. The right figures show the corresponding mean airflow maps and the path of the micro-drone. The centers of the area sources are denoted by crosses. The micro-drone started at position (27, 2) m. The concentration value of CO_2 is given in % by volume.

plume propagating in x direction can be identified in the produced predictive mean maps of trial #5. However, the source location is indicated perfectly by the high variance concentrations in four of the six predictive variance maps. An exception is, e.g., trial #1, where the high variance concentration is displaced approx. 3 m from the real source location. A reason for that could be here the missing last sweep (due to an exhausted battery). The IR gas sensor of the gas-sensing payload, however, has a considerably better spatial resolution over the area as it supports shorter response and decay times.

Inferno experiments – The experiments in the Inferno region were performed on two different days with different weather conditions. The first day was foggy with an average temperature of approx. 12°C and an average relative humidity of 77%. The average wind speed during the experiments was 0.4 m/s. No reliable statement concerning the degree of stability of the wind conditions can be made as the micro-drone measured consistently very low wind speeds that also could be interpreted as noise induced by the inaccuracies given by the GPS receiver of the micro-drone (that is part of the wind vector estimation approach). Altogether the weather conditions on the first day permitted higher gas accumulations close to the ground as no strong wind flow was present. The second day was sunny with an average temperature of almost 18°C and an average relative humidity of 58%. The average wind speed was in the range of approx. 1.1 to 1.3 m/s and the average wind direction was between 49° and 105°. The circular variance lay around 0.54 and 0.86. The stronger wind conditions of the second day likely enhance dispersion and dilution of the volcanic gases. Additionally, the significantly higher solar radiation produces convective currents, which further disperse and dilute the volcanic gases. Therefore, lower maximum concentration levels could be measured over the experimental area (see Fig. 3 comparing trial #1 and #3).
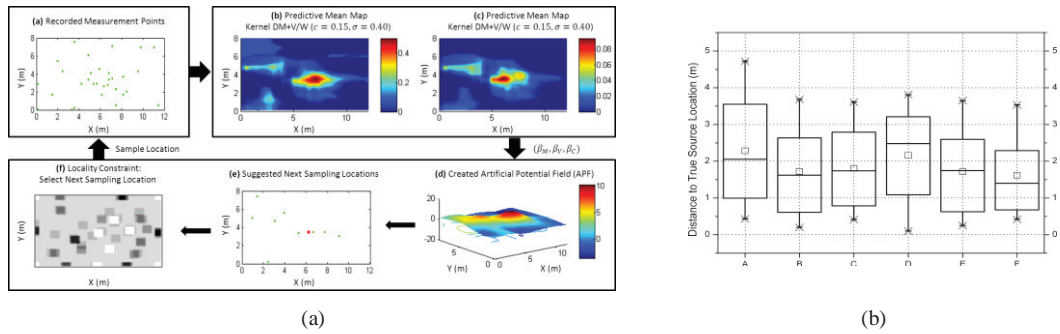
(a)	(b)

Fig. 4. **(a)** The adaptive sampling process: (a) from the previously visited sampling locations, (b) predictive mean and (c) variance maps were created using the Kernel DM+V/W algorithm. (d) Then, a set of next sampling points are selected from the created APF. (e) These points and the estimated source location are denoted by green and red dots, respectively. (f) The next sampling location is chosen based on the locality constraint sampling strategy (bottom, left), where the white cells are the previously selected cells and the darkest cells correspond to the most often suggested ones. All plots were created after the last time step of the SP algorithm. **(b)** Box-plot of the distance between the gas source location estimate and the true source location of the 16 runs after the last time step of the SP algorithm: A peak mean, B peak variance, C peak mean · variance, D mean, E variance, and F mean · variance. The box shows the lower/upper quartile and the line denotes the median. The mean is denoted by the small □. The x stands for outliers.

The results from the selected GDM experiments can be seen in Fig. 3. It seems that all created gas distribution maps reflect the area's gas emitting characteristics as the positions of the concentration rich areas correspond roughly to the naturally bubbling area sources. The qualitative results remain more or less comparable. This can especially be seen when comparing Fig. 3(a) and 3(b) from day 1. The quantitative results differ more strongly. The maximum concentration on day 1 (and day 2) decreases over time and added rotor disturbance. In Figs. 3(a) and 3(b), a drop in the maximum concentration from 3 to approx. 0.5 % by volume was detected, which strengthen the assumption made in [3] that the influence of the micro-drone's rotors cause dispersion with changing the magnitude and the position of the concentration maxima and that readjusting of the natural gas distribution needs time (depending on the release rate of the gas source). The first run probably has caused an alteration in the gas distribution. Additionally, the weather and wind conditions on the second day did not permit to repeat the high concentration measurements from the first day. This can be seen in Figs. 3(a) and 3(c).

Sensor planning experiments – The results presented in Fig. 4 demonstrate the suitability of the proposed SP algorithm for gas distribution mapping and its use for gas source localization. A total number of 16 runs were performed within this experiment. Fig. 4(b) shows for all 16 runs the distance between the true gas source location and six different estimates after the last measurement. The first three estimates are derived by selecting grid cells in which the predictive mean (A), predictive variance (B), or the product of mean and variance (C) are maximum. The forth estimate is derived by selecting grid cells in which the predictive mean (D) is larger than 90% of the maximum. The center of this area is taken as the source location estimate. In the same way the last two estimates are computed using the variance (E) or the product of mean and variance (F). The true source location was within the mean estimation area only in four trials and within the variance estimation area in six trials. This is in line with previous observations that the concentration variance often provides a better indication of the gas source location [6] than the mean. Initial results from these runs indicate the potential of adaptive sampling in providing a good estimate of the gas source location after a relatively small number of samples.

5. Conclusion and Future Work

Gas distribution modeling (GDM) by using an autonomous, flying, gas-sensitive micro-drone in uncontrolled environments is a challenging field of research. Even though the explored areas presented within this paper are not of considerable size, the application of the Kernel DM+V/W algorithm in combination with a gas-sensitive micro-drone is very promising with respect to the results of the presented real-world GDM experiments. Thus, micro-drones could be used to complement already existing monitoring infrastructure for CO_2 storage areas, and to increase the granularity of gas concentration measurements.

The first set of experiments in the geochemically active Tuscany region indicate that the micro-drone may not be suitable for *repeated* monitoring under low-wind conditions when quantitative reproducibility is needed since it introduces substantial disturbances to the gas distribution. The qualitative results still can be useful for identifying the gas source locations. However, the time between each mission has to be long enough to allow a recovery of the natural gas distribution. The second set of experiments indicates that qualitative and quantitative reproducibility depend on the stability of wind and weather conditions and that gas sensors with faster response times are required in order to reduce the measurement time and to be able to cover larger areas. However, one general problem is the memory effect in the sensor response due to the slow sensor recovery, which can be observed especially in the botanic garden experiments. Ishida et al. [7] proposed the integration of a sensor dynamics model to "reconstruct the actual gas distribution from the time-series response data considering the delay", which could reduce this effect. Furthermore, it is beneficial to use sensors with faster response and decay times for generating truthful representations of the gas dispersion. Multiple gas sources with different release rates might be hidden in the final gas distribution map, which makes the localization of these sources impossible. The approach of a multi-chamber e-nose (MCE-nose) proposed by Gonzalez et al. [8] could overcome this limitation as it "alternate[s] between sensing and recovery states [using redundant sensors], providing, as a whole, a device capable of sensing changes in chemical concentrations faster". In the third set of experiments, we applied a novel adaptive sampling strategy. The basic SP approach uses the statistical gas distribution models obtained with the Kernel DM+V/W algorithm. Areas of high mean and variance are good candidates for further inspection. Corresponding locations are prioritized through strong contributions to an APF. These exploitation contributions are balanced by repulsive contributions at previous sampling locations, which promote exploration. Our initial results with this extended SP algorithm show the potential of an adaptive sampling approach for GDM.

We also observe that the produced maps (and particularly the variance prediction) can provide good estimates of the gas source location. This is in line with previous observations that the concentration variance often provides a better indication of the gas source location [6] than the mean. Our initial conclusion when comparing sampling along a predefined sweeping trajectory with our proposed SP approach is therefore that with adaptive SP we tend to arrive more quickly at a meaningful map which allows to infer a reasonably accurate estimate of the gas source location. If the sampling device is a gas-sensitive micro-drone, as considered in this paper, then a strategy that avoids sampling at low-informative places is advantageous because of the resource constraints on the micro-drone. In addition, a lower number of measurements also tend to disturb the gas distribution less. This effect is, however, not taken into account in our current SP algorithm and we will investigate ways how to introduce a criterion that allows minimizing the degradation of the observed gas distribution through the micro-drone itself (e.g., by an additional criterion that prefers sampling locations in downwind direction).

The main limitations regarding the applicability of micro-drones for monitoring tasks of underground storage areas, especially CCS areas, can be summarized as follows:

- The rotor movement of the micro-drone influences the gas measurements. Thus, a lower limit of detection of CO_2 of approx. 0.2 to 0.5 % by volume is introduced.
- The flight time of approx. 20 *min* does not allow to perform monitoring tasks in large scale

scenarios with a single micro-drone. For example, a solution to the limited battery capacity would be to have a fleet of micro-drones that conduct the exploration task consecutively or in parallel.

- The slow response times of current gas sensors are also problematic for generating truthful representations of the gas dispersion. Furthermore, faster response times are required in order to reduce the measurement time and to be able to cover larger areas.
- The position uncertainty introduced by the GPS receiver of the micro-drone affects the accuracy of the gas distribution maps and the localization performance of the presented algorithms.

However, a measurement program to monitor CCS areas using micro-drones could include automated flights along predefined or adaptive trajectories at ground level once per day / night. Moreover, micro-drones could be used to enhance the spatial resolution of gas measurements and to locate leakages, when the permanently installed monitoring system triggers an alarm.

Acknowledgements

References

[1] Becker et al., "CCS - Environmental protection framework for an emerging technology," German Federal Environment Agency, 2009.

[2] Matthias Bartholmai and Patrick Neumann, "Multifunctional Sensor for Monitoring of CO_2 Underground Storage by Comprehensive and Spatially Resolved Measuring of Gas Concentrations, Temperature and Structural Changes," in Energy Procedia (GHGT-11), 2012.

[3] P. Neumann, S. Asadi, J. H. Schiller, A. J. Lilienthal, and M. Bartholmai, "Micro-Drone for Wind Vector Estimation and Gas Distribution Mapping," in IEEE Robotics and Automation Magazine, 2012, 19 (4), pages $50 - 61$.

[4] M. Bartholmai and P. Neumann, "Adaptive Spatial-Resolved Gas Concentration Measurement Using a Micro-Drone," in $tm - $ Technisches Messen, vol. 78, no. 10, pp. $470 - 478$, 2011.

[5] M. Reggente and A. J. Lilienthal, "Using Local Wind Information for Gas Distribution Mapping in Outdoor Environments with a Mobile Robot," in Proceedings of IEEE Sensors, 2009, pp. 1715–1720.

[6] A. Lilienthal and T. Duckett, "Creating gas concentration gridmaps with a mobile robot," in Proceedings of the IEEE/RSJ Int. Conf. on Intelligent Robots and Systems Las Vegas, NV, vol. 1, pp. $118 - 123$, 2003.

[7] H. Ishida, T. Nakamoto, and T. Moriizumi, "Remote sensing and localization of gas/odor source and distribution using mobile sensing system," in Proceedings of the International Conference on Solid State Sensors and Actuators , vol. 1, pp. $559 - 562$, 1997.

[8] J. Gonzalez-Jimenez, J. Monroy, and J. Blanco, "The Multi-Chamber Electronic Nose - An Improved Olfaction Sensor for Mobile Robotics," Sensors, vol. 11, no. 6, pp. $6145 - 6164$, 2011.